Contributions to the work function: A density-functional study of adsorbates at graphene ribbon edges

R. Ramprasad, Paul von Allmen, and L. R. C. Fonseca

Flat Panel Display Division (Motorola), 7700 South River Parkway, FPD22, Tempe, Arizona 85284

(Received 30 March 1999)

In the present computational study, we focus on graphene ribbons with zigzag edge atoms with their unsaturated bonds either dangling or terminated by various adsorbates (H, O, or Cs). Using this system as a test case, we discuss the two important contributions to the work function—the first one being an anisotropic bulk property related to the electron affinity of the material, and the second one being directly related to the surface dipole moment caused by the spill over of electronic charge into the vacuum. The latter contribution, which tends to increase the work function, can to a large extent be minimized by a judicious choice of adsorbates (typically, adsorbates that are more electropositive than the surface). The former face-dependent contribution turns out to be the minimum possible work function achievable for a given surface. Our calculations are based on density-functional theory within the local density approximation using nonlocal pseudopotentials and a plane wave basis set. [S0163-1829(99)03632-2]

I. INTRODUCTION

The work function, ϕ, of a crystal surface is defined as the energy needed to remove an electron at the Fermi level from the bulk region of a crystal to the vacuum at infinity.[1–3] ϕ, apart from describing the ability of an electron to escape from a material, correlates with the chemistry at the surface of a crystal. For instance, the work function is intimately related to the dipole barrier at the surface, and has been equated to the electronegativity in the case of elemental crystals (the electronegativity being the ability of one element to compete with others for the valence electronic charge during compound formation).[3,4] It is also well known that adsorption of species at a surface alters the work function of the surface in an understandable manner, with adsorbates having higher electronegativities than the surface increasing the work function while those with lower electronegativities having the opposite effect.[5–7]

In the present study, we quantify the above anticipated trends for the test case of graphene ribbon edges with various adsorbates. We also address an appealing—although not unanticipated—correlation between the edge dipole moment and the work function perpendicular to the edge (and along the ribbon plane). This correlation points to an interesting way of viewing the work function, *viz.*, by partitioning it into an anisotropic (face-dependent) bulk cohesive (electron affinitylike) part and a part entirely due to the surface or edge dipole moment. The latter, which is a positive contribution to the work function, is due to the spill over of the electron gas into the vacuum region, and can to a large extent be reduced by a judicious choice of adsorbates. In fact, this analysis indicates that there is a minimum possible work function associated with a particular surface or edge that can be attained when the surface or edge dipole moment can be made to vanish.

Our choice of an allotrope of carbon as a test case in the present study is motivated by the fact that recent attention has focused on carbon-based materials due to their promise

as potential candidates for cold-cathode field emission applications.[8] Among the allotropes of carbon, nanotubes seem to be active field emitters, although other forms—like fragments of graphene and diamond-like carbon—are also known to be active.[9] One possible reason the nanotubes are active may be because they display special electronic states localized at the tip atoms.[10,11] It has also been pointed out that the nanotubes may be quite defective, with one such defect being similar to a graphene edge.[12,13] While the carbon atoms in a cylindrical defect-free nanotube are all three-fold coordinated (just as in graphite), those in defected tubules may be two-fold coordinated, with an entirely different π-electron network in its vicinity (as in fragments of graphene). A recent tight-binding study of graphene ribbons[14] with the edge carbon atoms passivated with H has demonstrated that graphene ribbons with zigzag edges display special localized states near the Fermi level arising primarily due to the topology of the π electron networks at the edges. Here, we use density-functional methods and consider zigzag graphene edges with unsaturated bonds either dangling or passivated with H, O, or Cs, and assess the importance of such terminations on the edge dipole moment and the work function perpendicular to the edge—quantities which are key to the electron emission properties of these confined systems.

In the next section, we give details of the method and models used in this study. We comment about the specifics of the work function and dipole moment calculations and formally relate the former to the latter in Sec. III. In Sec. IV, we present electronic and geometric structure results, calculated work functions and dipole moments for the unpassivated and H-, O-, and Cs-terminated zigzag ribbons. We finally conclude with Sec. V.

II. MODELS AND METHOD

All calculations were performed using the local-density approximation[15,16] (LDA) within density-functional theory (DFT).[17,18] The electronic ground state was determined self-

consistently using the Teter-Payne-Allan preconditioned conjugate gradient method[19] through the solution of the Kohn-Sham single-particle equations, and the ionic positions were optimized using the Broyden-Fletcher-Goldfarb-Shano scheme[20] to minimize the Hellmann-Feynman forces.[21] A set of ''special'' points are used for the Brillouin-zone integrations,[22] along with a Fermi-Dirac broadening scheme,[23] to determine the Fermi level. Norm-conserving nonlocal pseudopotentials of the Troullier-Martins type,[24] transformed using the Kleinman-Bylander technique,[25] were used to describe C and O, with the pseudopotential parameters obtained from earlier work.[24] A Kleinman-Bylander transformed pseudopotential for Cs was generated using Vanderbilt's method[26] using core radii of 3.0 and 2.6 a.u. for the s and p components, respectively; the p potential was taken as the local component. For H, we used a local Troullier-Martins pseudopotential, with a core radius of 0.9 a.u.

A good test for the quality of a pseudopotential is its ability to reproduce equilibrium bulk properties; hence, bulk graphite and bcc Cs were considered. The equilibrium properties are determined by converging the results with respect to the plane wave cutoff energy and the number of **k** points used for sampling the Brillouin zone; convergence in the total energy was assumed to have been reached when the total energy was within 0.01 eV/atom of the well converged asymptotic value. For graphite, convergence was achieved when a 50 Ry plane wave cutoff and 18 special **k** points were used to sample quantities within the irreducible wedge of the Brillouin zone (IBZ). The calculated lattice constants ($a = 2.462$ Å and $c = 6.649$ Å) and cohesive energy (7.9 eV/atom) compare well with the corresponding experimental numbers ($a = 2.456$ Å, $c = 6.696$ Å, and $E_{coh} = 7.4$ eV/atom).[27,28] Convergence in the case of Cs was achieved at a plane wave cutoff energy of 10 Ry and 4 special **k** points. The calculated bcc lattice constant, cohesive energy, and bulk modulus are 6.105 Å, 0.855 eV, and 2.3 GPa, respectively, which are also in good agreement with experimental measurements (6.045 Å, 0.804 eV, and 2.0 GPa, respectively).[27,29] For O-terminated systems, we adopt a cutoff energy of 60 Ry, as used in earlier work involving O.[24]

Supercell slab geometries were assumed in treating graphene ribbons. All ribbon calculations were performed with four chains of carbon in each ribbon, and a vacuum of at least 12.0 Å in the direction perpendicular to the edge (calculations involving Cs required at least 20 Å of vacuum), and a vacuum of 5.0 Å perpendicular to the ribbon plane; Fig. 1 shows a schematic of the model system. The size of the vacuum region was chosen such that the self-consistent potential in the vacuum region flattens to its asymptotic value. As a result of the large size of the supercell, only six special **k** points within the surface IBZ were used for the ribbon calculations. All results presented here were well converged for the above choices of **k**-point mesh, slab, and vacuum thicknesses, and a plane wave cutoff energy of 50 Ry (60 Ry in O-terminated systems). Geometry optimizations were performed to determine surface relaxation. However, reconstructions of the atoms along the edges were not permitted due to the small size of the surface unit cell dictated by reasons of computational expediency; we anticipate edge reconstructions to result in only minor changes of the
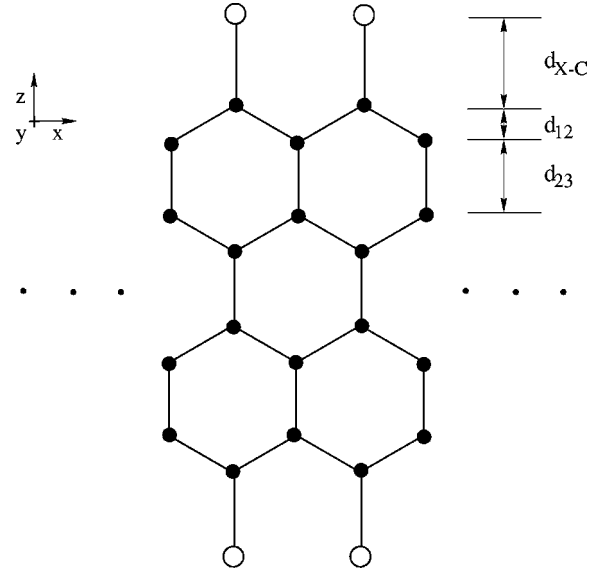

FIG. 1. Schematic of the zigzag graphene ribbon. Solid and open circles indicate carbon atoms and adsorbate (H, O, or Cs) atoms, respectively. The dots indicate periodicity along the x direction.

results reported here, with no changes in the qualitative trends. Geometries were assumed to be optimized when all forces were less than 0.03 eV/Å.

III. GENERAL COMMENTS ON WORK FUNCTION AND DIPOLE MOMENT CALCULATIONS

The work function is formally defined as

$$\phi = D - E_F, \tag{1}$$

where D is the electrostatic potential step at the surface (or the edge, in the present case), and E_F is the bulk Fermi energy, measured with respect to the average electrostatic reference potential.[3] The use of nonlocal pseudopotentials to treat the ion cores and the reciprocal-space formalism adopted in the present study restrict the choice of the reference potential. In the reciprocal-space formalism, there is an arbitrariness in the zero of the energy scale. The local pseudopotential and the Hartree potential for small wave vectors and the ion-ion interaction terms are individually divergent quantities, although they add up to a finite quantity.[30,31] The Kohn-Sham equations are hence solved by setting the $\mathbf{G}=0$ component of the local pseudopotential $[V_{loc}^{pp}(\mathbf{r})]$ and Hartree potential $[V_H(\mathbf{r})]$ to zero (as these contributions merely shift the band structure uniformly), introducing the arbitrariness mentioned above.[32] It should, however, be noted that although the actual value of the Fermi energy has no significance [since it has been shifted by an unknown amount equal to $V_H(\mathbf{G}=0) + V_{loc}^{pp}(\mathbf{G}=0)$], the Fermi energy *relative* to $V_H(\mathbf{r}) + V_{loc}^{pp}(\mathbf{r})$ is a well defined and transferable quantity. We thus adopt the following procedure to determine ϕ.

We calculate the planar-averaged potential $V_{avg}(z) = (\langle V_H(\mathbf{r}) + V_{loc}^{pp}(\mathbf{r}) \rangle_{XY})$ along the direction perpendicular to the edge for the graphene ribbon, i.e., planar-averaging is performed in the XY plane in Fig. 1. Independently, we de-
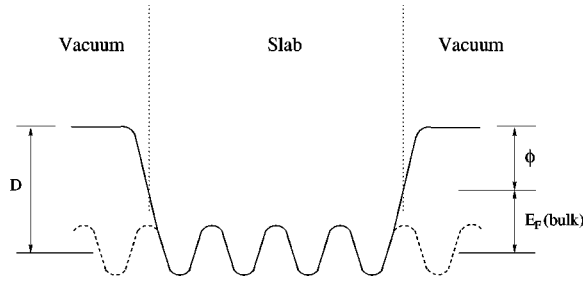
FIG. 2. Schematic of the planar-averaged potential $V_{avg}(z)$ for bulk (dashed line) and surface (solid line). E_F is the Fermi energy of the bulk. The planar-averaged potential for the surface is shifted so that it matches with the bulk potential. The work function ϕ for the surface is determined as the energy difference between the value of the (shifted) planar-averaged potential in the vacuum region and the bulk Fermi energy.
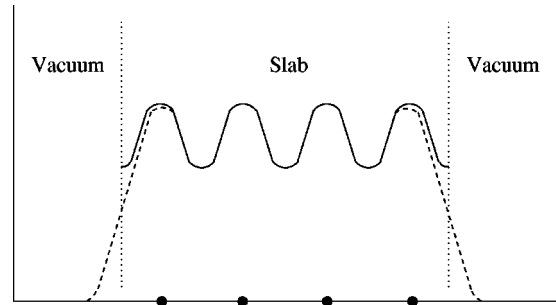

FIG. 3. Schematic of the planar-averaged electronic charge density for the reference system (solid line) and for the self-consistent situation (dashed line). Vertical dotted lines indicate surface truncation planes, and solid circles represent the location of the atom planes.

termine the same quantity (along the same direction) for an edgeless graphene sheet. We found that the former quantity in the interior regions of the ribbon is identical in shape to the latter (indicating bulklike behavior), although shifted by a constant amount. By matching up the two quantities, and by knowing the bulk Fermi energy relative to the bulk $V_{avg}(z)$, we calculate the work function as the difference between the surface $V_{avg}(z)$ in the vacuum region and the bulk Fermi energy.[7,33] We illustrate this schematically in Fig. 2.

We now comment on how ϕ can be intuitively partitioned into physically understandable components. For simplicity, let us ignore the relaxation of the surface ionic cores, which have been shown earlier to change ϕ negligibly.[33] Creation of a surface has two major implications: the first is a simple truncation of the material at the surface plane, and the second is the spill over into the vacuum region (or the self-consistent rearrangement) of electrons into the vacuum to minimize their kinetic energy. To be consistent with these ideas, let us decompose the electrostatic potential step D into two components, one purely a dipole effect due to the spill over of the electronic charge density into the vacuum region (say D_1), and the other due to the potential step in a ''reference'' system where there is no spill-over or rearrangement of charge (say D_2). The reference surface is composed of atoms with their electron densities frozen at their bulk values (i.e., bulk truncation for the ionic *and* electronic degrees of freedom, and the truncation is assumed to be performed exactly *between* adjacent planes). Figure 3 shows a schematic of the planar-averaged electronic charge density for both the hypothetical reference system and the self-consistent situation. The work function can then be written as

$$\phi = D_1 + (D_2 - E_F). \qquad (2)$$

$(D_2 - E_F)$ is purely an anisotropic material property, essentially a measure of the strength of the potential that binds an electron to the material (in other words, the electron affinity) and D_1 is a surface property that depends on the the spill over of electronic charge at the surface, and can change with the type of adsorbate on the surface, depending on how the adsorbate affects the surface dipole moment. Thus, changes in the work function of a surface due to various adsorbates are brought about by changes in D_1 *alone*. It should be noted

that our choice of the reference system yields orientation-dependent work functions, in contrast to other model systems composed of a superposition of atomic charge densities or bulk Wigner-Seitz unit cells used earlier.[33,34]

The exact relationship between D_1 (or ϕ) and the surface dipole moment can be seen to be a linear one by the following derivation. Consider a model slab system, whose surface is perpendicular to the z axis, filling the half-space $z \leq 0$. Let $\rho(x,y,z)$ be the deformation charge density, i.e., the difference between the charge density of the reference system with no charge spill over (where the surface or edge atom charge densities are identical to the bulk charge density) and the self-consistent charge density. $\rho(x,y,z)$ thus represents the redistribution of the charge density due to the creation of the surface or edge. The XY plane-averaged potential, $\bar{v}(z)$, induced by the dipole layer and the XY plane-averaged density, $\bar{\rho}(z)$, are related by Poisson's equation:

$$\frac{\partial^2}{\partial z^2}\bar{v}(z) = -4\pi\bar{\rho}(z), \qquad (3)$$

where

$$\bar{v}(z) = \frac{1}{A}\int\int v(x,y,z)dxdy; \qquad (4)$$

where A is the area of the surface unit cell, $v(x,y,z)$ is the potential induced due to the spill over, and the integrations are performed within the surface unit cell; a similar relationship holds for $\bar{\rho}(z)$. The solution of the above Poisson's equation with the boundary conditions given by vanishing potential and electric field at $z = +\infty$ is

$$\bar{v}(z) = -4\pi\int_z^\infty dz' z'\bar{\rho}(z') + 4\pi z\int_z^\infty dz'\bar{\rho}(z'). \qquad (5)$$

Since D_1 is given by $\bar{v}(\infty) - \bar{v}(-\infty)$, the work function can be written as

$$\phi = 4\pi\int_{-\infty}^\infty dz' z'\bar{\rho}(z') + (D_2 - E_F) = 4\pi\mu/A + (D_2 - E_F),$$
$$(6)$$

TABLE I. Selected geometric parameters, work functions (in eV) and edge dipole moments per unit surface area A (in eV) for the four-chain graphene ribbon for various cases of termination; see Fig. 1 for a description of geometric symbols.

	d_{12}	d_{23}	d_{X-C}	ϕ	μ/A
Clean	0.630	2.170		6.30	0.382
H-terminated	0.680	2.146	1.102	3.31	0.142
O-terminated	0.775	2.129	1.249	7.29	0.458
Cs-terminated	0.685	2.154	3.390	2.55	0.081
Unrelaxed, clean	0.719	2.130		6.34	0.383
Reference system	0.719	2.130		1.40	0.000

where we have assumed that the asymptotic form for the second integral of Eq. (5) is $1/z^{1+\epsilon}(\epsilon>0)$ for $z\rightarrow-\infty$, and the dipole moment for the surface unit cell along the z direction, μ, is defined as

$$\mu=\int_{-\infty}^{\infty}\int_{y}\int_{x}dx'dy'dz'z'\rho(x',y',z'), \qquad (7)$$

where the x and y integrations are performed within the surface unit cell. We thus see that the work function varies linearly with the dipole moment per unit area, with the slope being 4π, and the intercept being D_2-E_F. Therefore, an electron attempting to escape from a material has to surmount two barriers: a surface barrier (or the anisotropic electron affinity), D_2-E_F, that binds the electron to the bulk, and a dipole barrier entirely due to the surface dipole moment caused by the spill-over of the electronic charge density into the vacuum region. As we will see in the next section, any adsorbate that tends to decrease the extent of electronic spill over into the vacuum will decrease the work function of the system in that direction.

IV. RESULTS

Figure 1 shows a schematic of the model ribbon systems considered, and Table I lists the results for the variously terminated geometry optimized four-chain zigzag graphene ribbons; geometric parameters other than the ones listed in Table I changed by less than a percent from the corresponding bulk values. For comparison, we also list the results for the unoptimized (C atoms fixed at their bulk positions) clean four-chain zigzag ribbon. In order to ascertain that the electronic structure of the systems considered here is in agreement with the earlier tight-binding calculation,[14] we have calculated the band structure of the H-terminated graphene ribbon, which we show in Fig. 4. As in the earlier study,[14] we see a flat band close to the Fermi level close to the Brillouin zone boundaries; analysis of the charge density resulting from this band showed that the states responsible for the flat part of the band were localized at the edge atoms.

The work function perpendicular to the zigzag edge and the edge dipole moment per unit surface area are also listed in Table I. Interesting trends can be seen in the calculated work functions in Table I. The unpassivated, clean zigzag edge has a rather high work function of 6.3 eV. This value decreases drastically with H termination. O termination increases the work function and Cs termination decreases it to
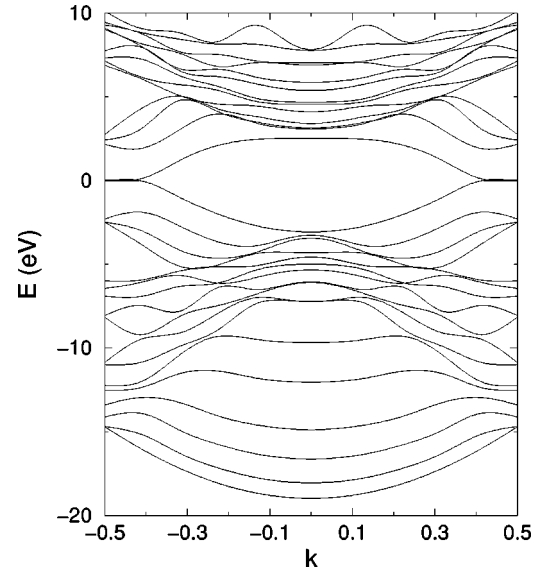

FIG. 4. Band structure of H-passivated zigzag graphene ribbon. The energy values shown are relative to the Fermi energy, and the k points are in units of $(2\pi/a)$, where a is the periodic length along the ribbon edge.

an even lower value than with H-termination. In general, we see that the more electropositive an adsorbate, larger is the work function decrease, consistent with results reported in the literature.[5–7] Changes in the dipole moment with adsorbates follow the work function changes. Clearly, adsorbates that are more electropositive than the surface, because of their propensity to lose electrons, cause an attenuation of the electronic charge spill over, decreasing the dipole moment, whereas more electronegative adsorbates enhance the spill over for the opposite reason.

Table I also lists the dipole moments, which are calculated relative to a hypothetical reference system where there is no leakage of the charge density from the edge into the vacuum (designated as reference in Table I); as mentioned earlier in Sec. III, the reference ribbon is composed of atoms
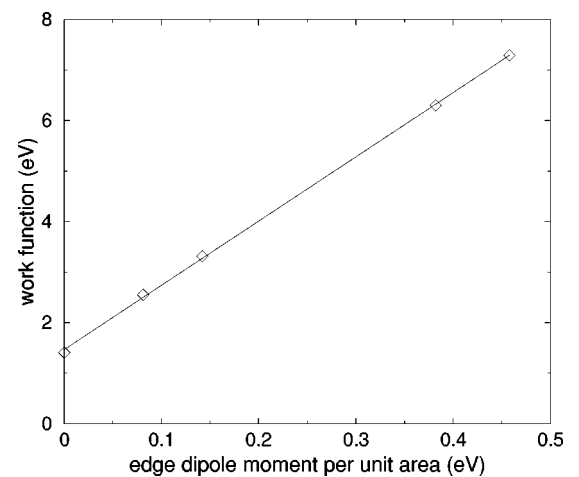

FIG. 5. Linear correlation between the work function and the edge dipole moment per unit area (last two columns of Table I) of the zigzag graphene ribbon for various terminations. The edge dipole moment is relative to a reference system for which there is no leakage of the electronic charge density into the vacuum.

with their electron densities frozen at their bulk values. As anticipated, a linear correlation exists (Fig. 5) between the work function and dipole moment (with an intercept corresponding to the work function of the reference system). The calculated slope of the plot is 12.72, in good agreement with the anticipated value of $4\pi(=12.57)$. Furthermore, Fig. 5 indicates that there exists a minimum possible theoretical work function corresponding to the situation when the surface dipole moment is zero (i.e., when there is absolutely no charge spill over into the vacuum); this minimum ϕ is, of course, $D_2 - E_F$ (defined in the previous section), an intrinsic anisotropic material property. In the case of the zigzag edge of graphene, the calculated minimum work function is 1.40 eV.

V. CONCLUSIONS

In the present study, we have identified two contributions to the work function of a surface—the first one being an anisotropic bulk property related to the electron affinity of the material, and the second one being directly related to the surface dipole moment caused by the spill over of electronic charge into the vacuum due to the creation of the surface. The latter contribution, which tends to increase the work function, can to a large extent, be minimized by a judicious choice of adsorbates (typically, adsorbates that are more electropositive than the surface). The former face-dependent contribution turns out to be the minimum possible work function achievable for a given surface. We have used the zigzag edges of graphene, with the edge atoms terminated with various adsorbates, as a test case in order to illustrate these concepts, and found that the minimum possible theoretical work function in the direction perpendicular to the zigzag edge (and along the graphene plane) is about 1.40 eV.

[1] E. Wigner and J. Bardeen, Phys. Rev. **48**, 84 (1935).

[2] N. D. Lang, in *Solid State Physics*, edited by F. Seitz and D. Turnbull (Academic, New York, 1973), Vol. 28, p. 225.

[3] M. Weinert and R.E. Watson, Phys. Rev. B **29**, 3001 (1984).

[4] W. Gordy, Phys. Rev. **69**, 604 (1946).

[5] A. Modinos, *Field, Thermionic and Secondary Electron Emission Spectroscopy* (Plenum, New York, 1984).

[6] R. Gomer, *Field Emission and Field Ionization* (Harvard University Press, Cambridge, 1961).

[7] Z. Zhang, M. Wensell, and J. Bernholc, Phys. Rev. B **51**, 5291 (1995).

[8] P.G. Collins and A. Zettl, Phys. Rev. B **55**, 9391 (1997).

[9] J. Robertson, Thin Solid Films **296**, 61 (1997).

[10] J. Bonard, J. Salvetat, T. Stöckli, W.A. de Heer, L. Forró, and A. Châtelain, Appl. Phys. Lett. **73**, 918 (1998).

[11] D.L. Carroll, P. Redlich, P.M. Ajayan, J.C. Charlier, X. Blase, A. de Vita, and R. Car, Phys. Rev. Lett. **78**, 2811 (1997).

[12] O. Zhou, R.M. Fleming, D.W. Murphy, R.C. Haddon, A.P. Ramirez, and S.H. Glarum, Science **263**, 1744 (1994).

[13] S. Amelinckx, D. Bernaerts, X.B. Zhang, G. van Tendeloo, and J. van Landuyt, Science **267**, 1334 (1995).

[14] K. Nakada, M. Fujita, G. Dresselhaus, and M.S. Dresselhaus, Phys. Rev. B **54**, 17 954 (1996).

[15] D.M. Ceperley and B.J. Alder, Phys. Rev. Lett. **45**, 566 (1980).

[16] J.P. Perdew and A. Zunger, Phys. Rev. B **23**, 5048 (1981).

[17] P. Hohenberg and W. Kohn, Phys. Rev. **136**, B864 (1964).

[18] W. Kohn and L.J. Sham, Phys. Rev. **140**, A1133 (1965).

[19] M.P. Teter, M.C. Payne, and D.C. Allan, Phys. Rev. B **40**, 12 255 (1989).

[20] D.F. Shano, Math. Op. Res. **3**, 244 (1978).

[21] R.P. Feynman, Phys. Rev. **56**, 340 (1939); H. Hellmann, *Einfuhrung in die Quantumchemie* (Deuticke, Leipzig, 1937).

[22] S. Froyen, Phys. Rev. B **39**, 3168 (1989).

[23] M. Weinert and J.W. Davenport, Phys. Rev. B **45**, 13 709 (1992).

[24] N. Troullier and J.L. Martins, Phys. Rev. B **43**, 1993 (1991).

[25] L. Kleinman and D.M. Bylander, Phys. Rev. Lett. **48**, 1425 (1982).

[26] D. Vanderbilt, Phys. Rev. B **32**, 8412 (1985).

[27] R. W. G. Wyckoff, *Crystal Structures*, 2nd ed. (Interscience Publishers, New York, 1963), Vol. 1.

[28] R.H. Baughman, H. Eckhardt, and M. Kertesz, J. Chem. Phys. **87**, 6687 (1987).

[29] C. Kittel, *Introduction to Solid State Physics* (Wiley, New York, 1976).

[30] W.E. Pickett, Comput. Phys. Rep. **9**, 115 (1989).

[31] J. Ihm, A. Zunger, and M.L. Cohen, J. Phys. C: Solid State Phys. **12**, 4409 (1979).

[32] The correct total energy of the system is later determined by adding the $V_H(\mathbf{G}=0) + V_{loc}^{pp}(\mathbf{G}=0) + E_{\text{ion-ion}}$ (which is a finite quantity, although each of the three components are individually divergent) to the total Kohn-Sham electronic energy (Refs. 30 and 31).

[33] C.J. Fall, N. Binggeli, and A. Baldereschi, Phys. Rev. B **58**, R7544 (1998).

[34] L.F. Mattheiss, Phys. Rev. **134**, 970 (1964).